Rolling Polyhedra on Tessellations

Akira Baes

Département d'Informatique, Université libre de Bruxelles, Belgium.

Erik D. Demaine

Computer Science and Artificial Intelligence Laboratory, Massachusetts Institute of Technology, USA.

Martin L. Demaine

Computer Science and Artificial Intelligence Laboratory, Massachusetts Institute of Technology, USA.

Elizabeth Hartung

Department of Mathematics, Massachusetts College of Liberal Arts, USA.

Stefan Langerman

Département d'Informatique, Université libre de Bruxelles, Belgium.

Joseph O'Rourke

Department of Computer Science, Smith College, Northampton, MA 01063, USA.

Ryuhei Uehara

School of Information Science, Japan Advanced Institute of Science and Technology, Japan.

Yushi Uno

Graduate School of Informatics, Osaka Metropolitan University.

Aaron Williams

Department of Computer Science, Williams College, USA.

Abstract

We study the possible moves and reachable space by *rolling* a 3D convex polyhedron on a 2D periodic tessellation in the xy-plane, where at every step a face of the polyhedron must coincide exactly with a tile of the tessellation it rests upon. We topple the polyhedron around one of the edges of the grounded face toward a neighboring face until it hits the xy-plane on a neighboring tile, only if the new face and the new tile also coincide. We observe the space that can be reached by succession of such rolling moves. If the whole plane can be reached, we call the polyhedron a *plane roller* for the given tessellation. We further classify polyhedra that only reach a limited strip or a bounded area on given tessellations as *band rollers* and *bounded rollers* respectively. We present a polynomial-time algorithm to determine the set of tiles reachable from a given starting position, which in particular determines the roller type of the given polyhedron and periodic tessellation. Using this algorithm, we compute the reachability for every regular-faced convex polyhedron on any regular-tiled (≤ 4)-uniform tessellation. Finally, we suggest how to employ these findings in puzzle games.

2012 ACM Subject Classification Theory of computation → Computational geometry; Theory of computation → Design and analysis of algorithms; Mathematics of computing → Discrete mathematics

Keywords and phrases polyhedra, tilings

Digital Object Identifier 10.4230/LIPIcs.FUN.2022.5

Funding *Elizabeth Hartung*: https://orcid.org/0000-0002-4041-1862
Stefan Langerman: Directeur de Recherches du F.R.S.-FNRS

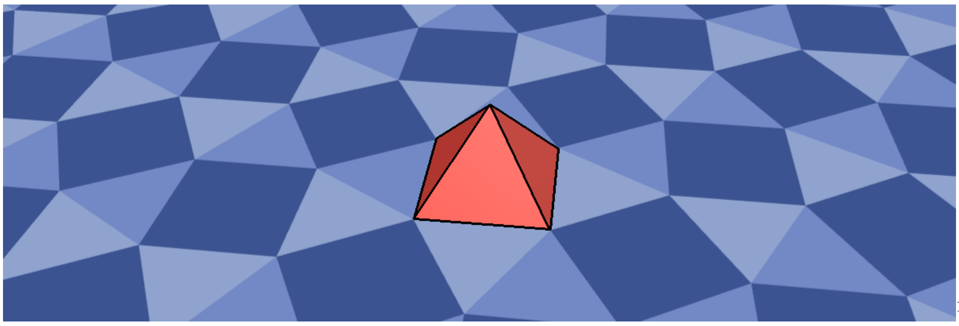
[1]

1 Introduction

When it comes to rolling a polyhedron, the cube has a monopoly in term of shape representation. *Dice rolling* puzzles feature a cube rolling around on the square grid. The goal is often to match a given face with a given tile. They were popularized by Martin Gardner [**g-mgsb-71**, **g-mc-77**, **g-tt-88**], but have seldom been generalized to other polyhedra on other grids, even though some pairings were known (see Figure 3). For perspective, rolling cubes on square grids are featured in a variety of computer games, such as *Korodice* (Gameboy, 1990), *Super Mario 64* (Nintendo 64, 1996), *Devil Dice* (Playstation, 1998), *Legacy of Kain: Soul Reaver* (Playstation, 1999), *Legend of Zelda Oracle of Ages* (Gameboy Color, 2001), *Bombastic* (Playstation 2, 2002), *Legend of Zelda Spirit Tracks* (Nintendo DS, 2009), *Rubek* (Windows, 2016), *Roll The Box* (Mobile, 2021), and *The Last Cube* (Windows, 2022); see Figure 1. *HyperRogue* (Windows, 2015) on the other hand involves hexagonal and heptagonal tiles in a hyperbolic space, and in its 2021 update, rolling tetrahedron, octahedron, or icosahedron dice on a triangular lattice. With various constraints, these puzzles can be NP-complete [**buchin2007rolling**, **j-dice**]; when rolling more shapes, they can be PSPACE-complete [**buchin2012rolling**, **holzer2012complexity**].

We formalize the concept of rolling any convex regular-faced 3D polyhedron P on any regular-tiled periodic tessellation T, which we imagine as lying in the (horizontal) xy-plane. Recall that a regular-faced convex polyhedron has regular polygons as faces, and that a plane tessellation is a partition of the plane into a collection T of polygons called *tiles* [**Grunbaum-1987**]. A regular-tiled tessellation has regular polygons as tiles. When a tile of T is congruent to a face of P, we call them *compatible*.

To start, we place the polyhedron P on the tessellation so that one of its faces *rests* (i.e., coincides exactly) with a compatible tile. In a *rolling step*, we rotate the polyhedron about one of the edges of its resting face, until another face rests on the tessellation. For the roll to be *valid*, we insist that, at the end of the motion, the adjacent face of P across the rolling edge rests on another (adjacent) compatible tile. See Figure 4 for an example.

Valid sequences of rolls form paths in the *rolling graph* of possible configurations. If the rolling graph contains a connected component that includes every tile of T, then we call the polyhedron a *plane roller* for that tessellation and starting position, as it can eventually roll to cover the entire plane.

[1] Screenshot from `https://polyhedra.veille-attitude.com/`, a 3D rolling visualisation program made on the subject of this article by Rachel Aouad Albashara, Luca Insisa, Quentin Magron, Dan Ngongo, Dang Phi L Pham and Simon Yousfi for the *ULB* Comupter Sciences Bachelor *Printemps des Sciences* showcase.

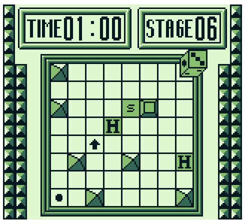

(a) *Korodice* (1990)

(b) *Zelda Oracle of Ages* (2001)

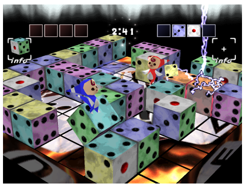

(c) *Devil Dice* (1998) [screenshot: thebobble]

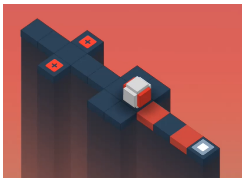

(d) *Rubek* (2016)

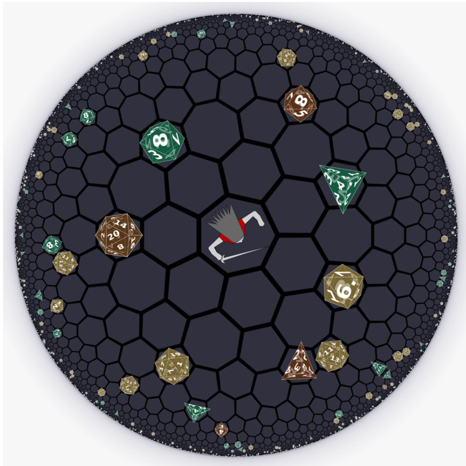

(e) *HyperRogue* (2015) Dice Reserve update (2021)

Figure 1 Cube and dice-rolling puzzles in video games.

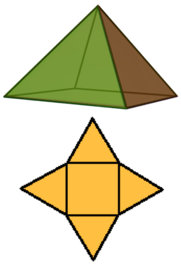

(a) Pyramid with its net made of regular polygons.

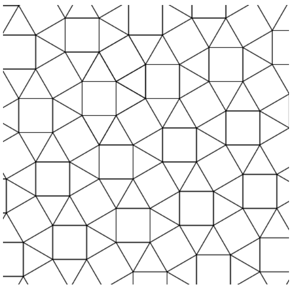

(b) The snub squares tiling made of regular triangles and squares.

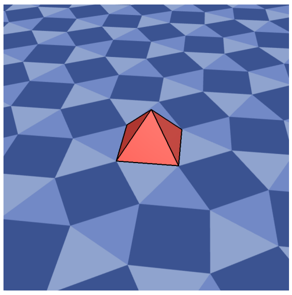

(c) Pyramid sitting on a compatible (congruent) tile on the tiling.

Figure 2 A polyhedron and a compatible tessellation are required for rolling.

1.1 Our results.

In this paper, we develop a polynomial-time algorithm to identify if a polyhedron with a periodic tessellation on a starting location is a plane roller. We essentially take advantage of

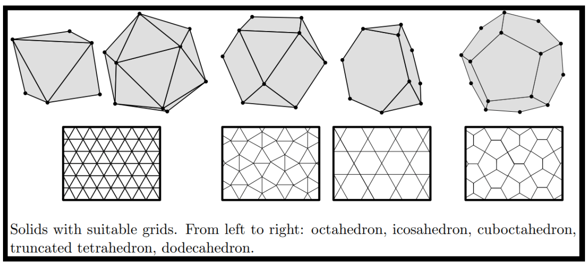

Figure 3 Tiling/polyhedron pairs considered suitable for games by Buchin et al. [**buchin2007rolling**]

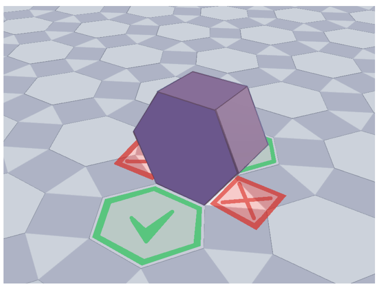

Figure 4 Valid and invalid rolls. Invalid rolls are forbidden moves.

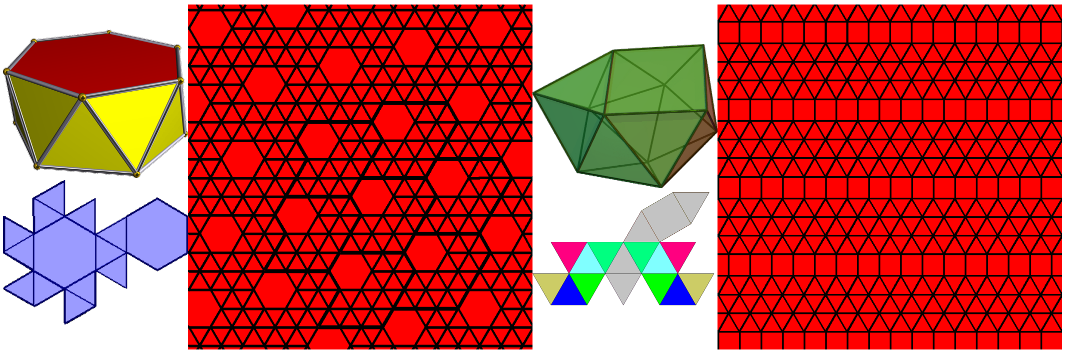

(a) hexagonal antiprism on $(3^6; 3^4x6)_2$ **(b)** J87 on $(3^6; 3^3x4^2)_2$

Figure 5 Examples of reachable area patterns generated by *plane rollers* (full cover).

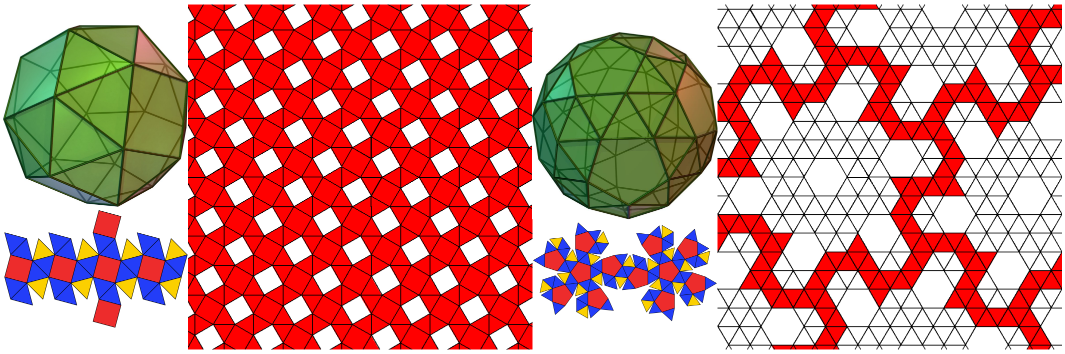

(a) snub cube on $(3^2x4x3x4)$ **(b)** snub dodecahedron on $(3^6; 3^4x6)_2$

Figure 6 Examples of reachable area patterns generated by *hollow-plane rollers* which leave holes in the plane.

the periodicity of the tessellations, coupled with the structure of the polyhedron, to prove that the resulting rolling graph also has a periodic structure that we can exploit.

We then apply this algorithm to completely categorize a natural finite set of interesting special cases; see Figure 11. For polyhedra, we consider the *regular-faced* convex polyhedra: the 5 Platonic solids [**euclid300BCE_elements**], 13 Archimedean solids [**field1997rediscovering**], 92 Johnson solids and their chiral variations [**grunbaum1965faces**, **johnson1966convex**, **zalgaller1967convex**], and n-prisms and n-antiprisms where $n \in \{3, 4, 6, 8, 10, 12\}$, as higher-sided polygons cannot be used to tile the plane [**Grunbaum-1987**]. For plane tessellations, we consider all k-uniform tilings for $k \geq 4$, as listed in [**chavey1989tilingscatalog**] and defined below. Including chiral variations, this makes 129 polyhedron nets to test on 131 tilings. For each case, we characterize the polyhedron rolling on the tessellation as *plane rollers* which cover the whole plane, *hollow-plane rollers* which cover a plane while leaving holes, *band rollers* which cover an infinite band, and *bounded rollers* which are confined to a finite area; see Figures 5,6,7,8 for several examples and Table 1 for a condensed view of the results. The most important result is the list of 145 plane roller pairs that we have found, which have uses in rolling puzzle games as alternatives to the classical cube-and-square-tiling pairing.

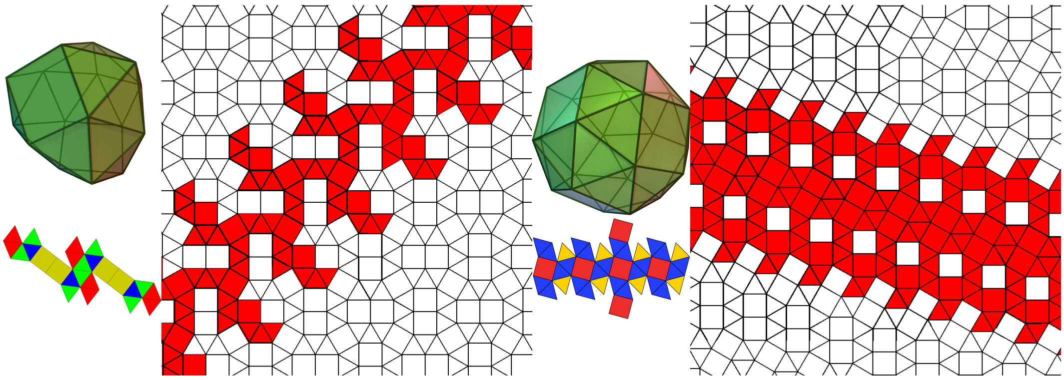

(a) J90 on $(3^3x4^2; 3^2x4x3x4)_1$ **(b)** snub cube on $(3^3x4^2; 3^2x4x3x4)_2$

Figure 7 Examples of reachable areas patterns generated by *band rollers* which is stuck in an infinite band extending from the starting position.

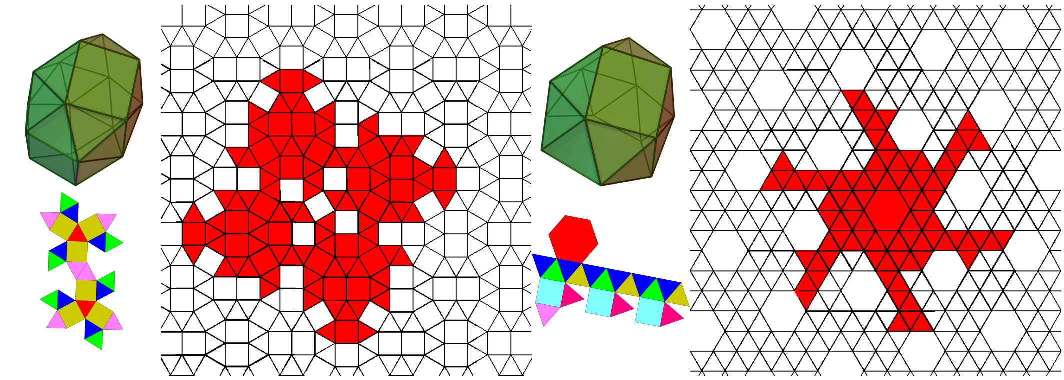

(a) J44 on $(3^3x4^2; 3^2x4x3x4)_1$ **(b)** J22 on $(3^6; 3^4x6)_2$

Figure 8 Examples of reachable area patterns generated by *bounded rollers* where the polyhedron is stuck in its starting area.

1.2 Definitions

As we require descriptions of regular-tiled tessellations to work with, recall that k-uniform tilings can be defined as follows. A tiling whose polygons are aligned edge-to-edge can be seen as a *primary graph* whose vertices are the points where tile corners join, and whose edges are the shared edges between pairs of tiles. A *vertex type* is the clockwise cyclic order of type of tiles (polygon shape) that surround a vertex [**chavey1989tilingscatalog**]. A tiling that contains k orbits of vertex types that transitively describe all of its tiles through k symmetry groups is a k-*isogonal* tiling. If a k-isogonal tiling uses regular polygons as tiles, then it is called k-*uniform*. Vertex types of k-uniform tessellations can be written as the list of the number of sides of the regular polygons of the tiles surrounding the vertices. See Figure 9. It is thus conventional to simply name unique k-uniform tilings by the list of their vertex types, and overlapping names are differentiated through a subscript.

Working with vertex types can be unwieldy, so we also describe the tilings as explorable graphs. All k-uniform tessellations are *periodic* on their vertices and on their faces, according to two translational symmetries and a fundamental domain called a "supertile." See Figure 10 for an example. A k-isogonal tiling is also n-isohedral for some $n \geq k$ [**chavey1989tilingscatalog**]

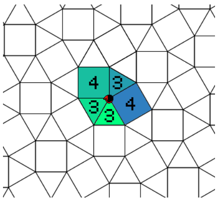

(a) $(3^2 * 4 * 3 * 4)$
1-uniform tiling
(archimedean)

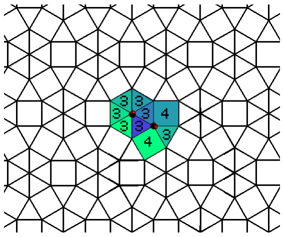

(b) $(3^6; 3^2 * 4 * 3 * 4)$
2-uniform tiling

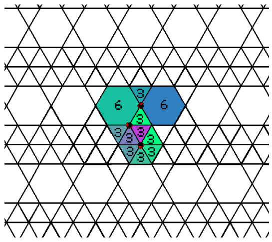

(c) $(3^6; 3^4 * 6; 3 * 6 * 3 * 6)$
3-uniform tiling

Figure 9 Examples of the naming convention of uniform tilings in the standardized "isogonal vertex type" notation, each point belonging to an orbit describing vertex types around it.

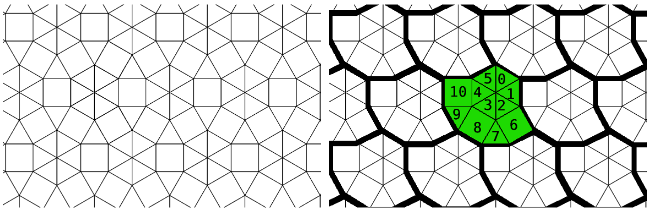

Figure 10 The same tiling as Figure 9b $(3^6; 3^2 * 4 * 3 * 4)$ in its supertile tiling representation.

meaning that, in the dual graph of the tiling whose nodes are tiles and edges define neighbors, there are n orbits of tiles that transitively describe all of its tiles through k symmetry groups [**chavey1989tilingscatalog**]. This means our k-uniform tessellations are formed by $n \geq k$ transitive classes of translations, rotations, and mirror symmetries that can tile the plane by copies of their starting tile, called *prototiles*. We can merge the prototile with its mirror symmetry if there is one, and merge with all of its rotations if there is rotational symmetry. (In a k-uniform tessellation, there are at most 12-wise rotations of 30° because of the limitations of regular polygons.) The result is a *parallelogon supertile* that has two translation symmetries (only) defining the tessellation [**Grunbaum-1987**]. In our case, it was quicker to describe the supertiles of each tiling by hand in a homemade periodic tessellation drawing tool, as we had no automated algorithm on hand to convert vertex-type orbits (isohedral, edges) notations to dual-graph supertile (isogonal, tiles) notations, but we had access to a list of n-uniform tessellation drawings on which we applied the above method. This is why we limited ourselves to (≤ 4)-uniform tilings, which still cover 131 of the most commonly found periodic tilings.

1.3 Related work

Rolling a polyhedron to cover the space in some form has been explored in [**chitour1997rolling**], in term of reachability in space in [**bicchi2004reachability**]. We are specifically interested in work that used the faces of the polyhedron as a base for a tessellation. Akiyama [**akiyama2007tile**] defined a *frame-stamper* as a regular polyhedron that covers the whole plane with a tiling by rolling in arbitrary directions stamping its face on the plane, and a *tile-maker* as a polyhedron whose net developments all generate a tiling pattern. A more relaxed definition in [**akiyama2010determination**] determines all *tessellation polyhedra* — regular-faced convex polyhedra that have at least one net development that can be used to tile the plane.

Polyhedrons that Roll on a Plane on a given tessellation: (42 results for 145 pairings)

tetrahedron with (3^6) – **cube** with (4^4) – **octahedron** with (3^6) – **icosahedron** with (3^6) – **truncated tetrahedron** with $(3^6; 3^2.6^2)$ – **cuboctahedron** with $(3^2.4.3.4)$, $(3^6; 3^2.4.3.4)$, $(3^3.4^2; 3^2.4.3.4)1$, $(3^6; 3^2.4.3.4; 3^2.4.3.4)$ – **j1** with $(3^2.4.3.4)$, $(3^6; 3^2.4.3.4)$, $(3^3.4^2; 3^2.4.3.4)1$, $(3^6; 3^3.4^2; 3^2.4.3.4)$, $(3^6; 3^2.4.3.4; 3^2.4.3.4)$ – **j3** with $(3^6; 3^2.4.3.3.4; 3.4^2.6)$, $(3^6; 3^2.4.3.4; 3.4^2.6; 3.4.6.4)$ – **j8** with (4^4), $(3^6; 3^3.4^2; 4^4)1$, $(3^6; 3^3.4^2; 4^4)3$, $(3^6; 3^3.4^2; 3^2.4.3.4; 4^4)$ – **j10** with (3^6), $(3^6; 3^3.4^2)1$, $(3^6; 3^3.4^2)2$, $(3^6; 3^2.4.3.4)$, $(3^6; 3^3.4^2; 3^2.4.3.4)$, $(3^6; 3^6; 3^3.4^2)1$, $(3^6; 3^6; 3^3.4^2)2$, $(3^6; 3^3.4^2; 3^2.4.3.4; 4^4)$ – **j11** with (3^6) – **j12** with (3^6) – **j13** with (3^6) – **j14** with $(3^6; 3^3.4^2)1$ – **j15** with $(3^6; 3^3.4^2)1$ – **j16** with $(3^6; 3^3.4^2)1$ – **j17** with (3^6) – **j22** with $(3^6; 3^4.6)1$, $(3^6; 3^4.6; 3.6.3.6)2$, $(3^6; 3^4.6; 3.6.3.6)3$, $(3^6; 3^6; 3^4.6^2)$ – **j26** with $(3^2.4.3.4)$, $(3^3.4^2; 3^2.4.3.4)2$, $(3^6; 3^2.4.3.4; 3^2.4.3.4)$ – **j27** with $(3^3.4^2)$, $(3^3.4^2; 3^2.4.3.4)1$, $(3^6; 3^3.4^2; 3^2.4.3.4)$, $(3^3.4^2; 3^2.4.3.4; 3^2.4.3.4)$ – **j28** with $(3^3.4^2)$, $(3^3.4^2; 4^4; 4^4)1$ – **j29** with $(3^2.4.3.4)$, $(3^6; 3^2.4.3.4; 3^2.4.3.4)$ – **j30** with $(3^3.4^2)$ – **j31** with $(3^2.4.3.4)$, $(3^6; 3^2.4.3.4; 3^2.4.3.4)$ – **j37** with (4^4) – **j44** with $(3^6; 3^2.4.3.4; 3^2.4.3.4)$, $(3^3.4^2; 3^2.4.3.4; 3^2.4.3.4)$ – **j44 chiral** with $(3^6; 3^2.4.3.4; 3^2.4.3.4)$ – **j50** with (3^6), $(3^6; 3^3.4^2)1$, $(3^6; 3^3.4^2)2$, $(3^6; 3^2.4.3.4)$, $(3^6; 3^6; 3^3.4^2)1$, $(3^6; 3^6; 3^3.4^2)2$, $(3^6; 3^3.4^2; 3^2.4.3.4; 4^4)$ – **j51** with (3^6) – **j54** with $(3.4.6.4)$ – **j56** with $(3.4.6.4)$ – **j62** with (3^6) – **j65** with $(3.6.3.6)$ – **j84** with (3^6) – **j85** with (3^6), $(3^6; 3^3.4^2)1$, $(3^6; 3^3.4^2)2$, $(3^6; 3^2.4.3.4)$, $(3^6; 3^6; 3^3.4^2)1$, $(3^6; 3^6; 3^3.4^2)2$, $(3^6; 3^3.4^2; 3^3.4^2)1$, $(3^6; 3^3.4^2; 3^3.4^2)2$, $(3^6; 3^3.4^2; 3^2.4.3.4; 4^4)$ – **j86** with (3^6), $(3^6; 3^3.4^2)1$, $(3^6; 3^3.4^2)2$, $(3^6; 3^2.4.3.4)$, $(3^6; 3^3.4^2; 3^2.4.3.4)$, $(3^6; 3^3.4^2; 4^4)1$, $(3^6; 3^3.4^2; 4^4)2$, $(3^6; 3^6; 3^3.4^2)1$, $(3^6; 3^6; 3^3.4^2)2$, $(3^6; 3^3.4^2; 3^2.4.3.4; 4^4)$ – **j87** with (3^6), $(3^6; 3^3.4^2)1$, $(3^6; 3^3.4^2)2$, $(3^6; 3^2.4.3.4)$, $(3^6; 3^6; 3^3.4^2)1$, $(3^6; 3^6; 3^3.4^2)2$, $(3^6; 3^3.4^2; 3^2.4.3.4; 4^4)$ – **j88** with (3^6), $(3^6; 3^3.4^2)1$, $(3^6; 3^3.4^2)2$, $(3^6; 3^3.4^2; 3^2.4.3.4)$, $(3^6; 3^3.4^2; 4^4)1$, $(3^6; 3^3.4^2; 4^4)2$, $(3^6; 3^6; 3^3.4^2)1$, $(3^6; 3^6; 3^3.4^2)2$, $(3^6; 3^3.4^2; 3^3.4^2)1$, $(3^6; 3^3.4^2; 3^3.4^2)2$ – **j89** with (3^6), $(3^6; 3^3.4^2)1$, $(3^6; 3^3.4^2)2$, $(3^6; 3^2.4.3.4)$, $(3^6; 3^3.4^2; 3^2.4.3.4)$, $(3^6; 3^3.4^2; 4^4)3$, $(3^6; 3^3.4^2; 4^4)4$, $(3^6; 3^6; 3^3.4^2)1$, $(3^6; 3^6; 3^3.4^2)2$, $(3^6; 3^3.4^2; 3^3.4^2)1$, $(3^6; 3^3.4^2; 3^3.4^2)2$ – **j90** with (3^6), $(3^6; 3^3.4^2)1$, $(3^6; 3^3.4^2)2$, $(3^6; 3^2.4.3.4)$, $(3^6; 3^3.4^2; 3^2.4.3.4)$, $(3^6; 3^3.4^2; 4^4)1$, $(3^6; 3^3.4^2; 4^4)2$, $(3^6; 3^6; 3^3.4^2)1$, $(3^6; 3^6; 3^3.4^2)2$, $(3^6; 3^3.4^2; 3^3.4^2)1$, $(3^6; 3^3.4^2; 3^3.4^2)2$, $(3^6; 3^2.4.3.4; 3^2.4.3.4)$, $(3^6; 3^3.4^2; 3^2.4.3.4; 4^4)$ – **square antiprism** with $(3^3.4^2)$ – **hexagonal antiprism** with $(3^4.6)$, $(3^6; 3^4.6)1$, $(3^6; 3^4.6)2$, $(3^4.6; 3^2.6^2)$, $(3^6; 3^4.6; 3^2.6^2)2$, $(3^6; 3^4.6; 3.6.3.6)1$, $(3^6; 3^4.6; 3.6.3.6)2$, $(3^6; 3^4.6; 3.6.3.6)3$, $(3^6; 3^6; 3^4.6^2)$, $(3^6; 3^4.6; 3^4.6)$, $(3^4.6; 3^4.6; 3.6.3.6)1$, $(3^4.6; 3^4.6; 3.6.3.6)2$, $(3^6; 3^4.6; 3^2.6^2; 3.6.3.6)$, $(3^4.6; 3^2.6^2; 3^2.6^2; 3.6.3.6)$

Polyhedrons that Roll on a Hollow plane on a given tessellation: (76 results for 588 pairings)

tetrahedron (x7) - octahedron (x7) - icosahedron (x7) - truncated tetrahedron (x12) - cuboctahedron (x4) - truncated cube - truncated octahedron (x10) - rhombicuboctahedron (x8) - truncated cuboctahedron (x6) - snub cube (x13) - snub cube chiral (x12) - truncated icosahedron (x4) - rhombicosidodecahedron (x4) - truncated icosidodecahedron (x5) - snub dodecahedron (x5) - snub dodecahedron chiral (x4) - j1 (x6) - j3 (x8) - j7 (x5) - j8 - j10 (x15) - j11 (x6) - j12 (x7) - j13 (x7) - j14 (x15) - j15 (x15) - j16 (x15) - j17 (x7) - j18 (x7) - j19 (x4) - j22 - j26 (x2) - j27 (x13) - j28 (x8) - j29 (x2) - j30 (x6) - j31 - j35 (x11) - j37 (x3) - j38 (x7) - j44 (x6) - j44 chiral (x5) - j45 (x2) - j45 chiral (x2) - j49 (x8) - j50 (x16) - j51 (x7) - j53 (x6) - j54 (x14) - j55 (x10) - j56 (x16) - j57 (x14) - j62 (x4) - j65 (x3) - j66 - j72 (x4) - j74 (x10) - j75 (x6) - j76 (x4) - j78 (x4) - j79 (x6) - j81 (x4) - j84 (x7) - j85 (x16) - j86 (x16) - j87 (x18) - j88 (x18) - j89 (x20) - j90 (x16) - triangular prism (x12) - hexagonal prism (x18) - octagonal prism - dodecagonal prism (x4) - square antiprism (x5) - hexagonal antiprism (x2) - dodecagonal antiprism (x2)

Polyhedrons that Roll on a Band on a given tessellation: (94 results for 2623 pairings)

tetrahedron (x35) - cube (x41) - octahedron (x35) - icosahedron (x35) - truncated tetrahedron (x34) - cuboctahedron (x3) - truncated octahedron (x15) - rhombicuboctahedron (x43) - snub cube (x7) - snub cube chiral (x8) - truncated icosahedron (x13) - rhombicosidodecahedron (x2) - snub dodecahedron (x7) - snub dodecahedron chiral (x7) - j1 (x7) - j3 (x2) - j7 (x43) - j8 (x39) - j9 (x42) - j10 (x29) - j11 (x31) - j12 (x35) - j13 (x35) - j14 (x42) - j15 (x42) - j16 (x42) - j17 (x35) - j18 (x43) - j19 (x41) - j20 (x42) - j21 (x42) - j22 (x30) - j23 (x30) - j24 (x30) - j25 (x30) - j26 (x7) - j27 (x17) - j28 (x46) - j29 (x4) - j30 (x15) - j31 (x3) - j35 (x44) - j36 (x49) - j37 (x46) - j38 (x44) - j39 (x47) - j40 (x42) - j41 (x42) - j42 (x42) - j43 (x42) - j44 (x32) - j44 chiral (x33) - j45 (x31) - j45 chiral (x32) - j46 (x32) - j46 chiral (x32) - j47 (x30) - j47 chiral (x30) - j48 (x30) - j48 chiral (x30) - j49 (x20) - j50 (x27) - j51 (x35) - j54 (x8) - j55 (x10) - j56 (x15) - j57 (x11) - j62 (x17) - j65 (x25) - j67 - j72 - j73 (x5) - j76 - j77 (x5) - j80 (x5) - j84 (x35) - j85 (x32) - j86 (x27) - j87 (x28) - j88 (x23) - j89 (x21) - j90 (x25) - triangular prism (x45) - pentagonal prism (x42) - hexagonal prism (x36) - octagonal prism (x42) - decagonal prism (x42) - dodecagonal prism (x43) - square antiprism (x37) - pentagonal antiprism (x30) - hexagonal antiprism (x40) - octagonal antiprism (x30) - decagonal antiprism (x30) - dodecagonal antiprism (x30)

Table 1 Polyhedrons found in each Roller classification with impacted Tessellations pairing count.

Figure 11 Screenshot of the rolling pair reachable areas classification clickable web-table available at `https://akirabaes.com/polyrolly/resulttable/` in full.

2 Classification algorithm

General outline:

We describe a polyhedron as a dual graph (net of faces). We describe a tiling as an infinite dual graph (tiles). We focus on periodic tilings that can be described as a repeated structure (supertile) and a set of two coordinates. We create a looping multigraph from the supertile, and we keep track of (i,j) the supertile coordinates when leaving its boundaries. This allows us to more easily explore the plane. We join the polyhedron's net graph and the tessellation's multigraph while keeping track of their relative orientation. We describe a state (f, t, o) of the rolling graph as a face in the polyhedron's graph, a tile in the supertile graph and their relative orientation. A position in the rolling graph is $< (i, j), (f, t, o) >$. We explore a

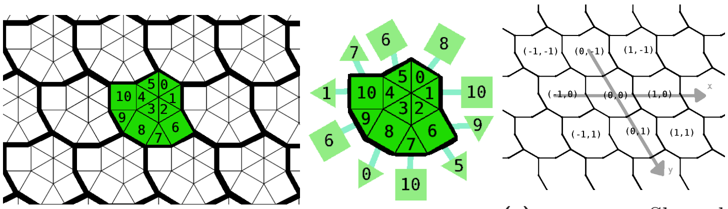

(a) The periodic tiling and the supertile described on it.

(b) The supertile graph.

(c) Skewed coordinates system over supertiles.

Figure 12 Infinite tiling to supertile multigraph

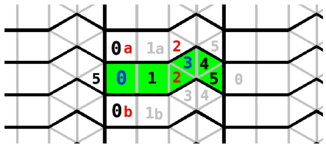

Figure 13 Tiling where a multigraph is necessary. See tiles 3 and 2.

limited amount of steps away in a connected component of the rolling graph to find repeated states of the connected component through the pigeonhole principle. From this as a basis, we find the linearly independent symmetry vectors of the periodic structure of the connected component over the rolling graph.

We can determine that the polyhedron/tessellation pairing is not a plane roller if we find only zero or one linearly independent symmetry vectors. If the reachable area has two symmetry vectors, we can determine that it is a periodic graph.

In a second step, we can describe the rolling graph's connected component's graph as a repeated structure (representative area) framed by the symmetry vectors to create a smaller looping rolling graph. We exhaustively explore the tiles of this closed graph to prove whether or not every tile in the tessellation can be reached by rolling.

2.1 Tilings

There is an uncountable infinity of tilings, even when using only unit square tiles. We restrict our attention to *periodic tilings*. These have two linearly independent translational symmetries (say, $\vec{a}$ and $\vec{b}$) and can be described by a *fundamental domain* for the action of these symmetries. The fundamental domain is a connected subset of the tiles (one for each orbit), which glued together form a *supertile* S. We denote by $|S|$ the number of tiles in the supertile. The supertile (and the tiles that compose it) can be repeated by the action of the two translations to obtain the original tiling. As S tiles the plane isohedrally by translation, its boundary can be decomposed into six pieces, denoted by $A, B, C, \bar{A}, \bar{B}, \bar{C}$, counterclockwise, where $\bar{A}$, $\bar{B}$, and $\bar{C}$ are translations of A by the action of $\vec{a}$, B by the action of $\vec{b}$, and C by the action of $\vec{b}-\vec{a}$, respectively.

A copy of the supertile can be identified by its integer coordinates in the *basis* formed by the translation vectors $\vec{a}$ and $\vec{b}$. That is, the copy (i,j) corresponds to the application of the translation $i\vec{a}+j\vec{b}$ to S. An individual tile t of the tiling T can then be uniquely identified by $\langle(i,j),s\rangle$: the coordinates (i,j) of the copy of S it is located in and its representative tile s within S.

A tiling T can also be represented by its (infinite) dual graph[2] G_T, where each tile is a vertex of G_T, and two vertices are connected by an edge if the two corresponding tiles are adjacent. When T is a periodic tiling, it is represented by the dual multigraph G_S of its supertile S. For tiles touching the boundary of S, we connect them to the tiles to which they are adjacent in the other copy or copies of the supertile, and mark the dual edges by A,B,C,$\bar{A}$,$\bar{B}$, or $\bar{C}$ depending on the portion of the boundary they cross. The graph G_S is the

[2] This can be a multigraph, with parallel edges when two tiles are adjacent on more than one edge.

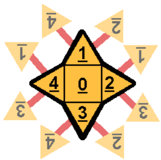

Figure 14 Dual graph of a pyramid with information about the relative orientations of its faces.

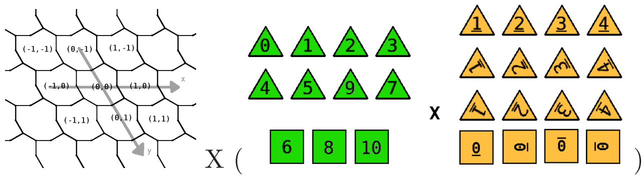

Figure 15 The rolling graph is composed of $< (i,j), (tile, face, orientation) >$

quotient of G_T by the action of the symmetries $\vec{a}$ and $\vec{b}$ (also denoted $G_T/\{\vec{a},\vec{b}\}$). The graph G_S can be used to navigate the tiling T or the graph G_T by updating the representation $\langle (i,j), s\rangle$ when moving to an adjacent tile. The tile s is updated to the adjacent tile s' in G_S, and the coordinates (i,j) need to be updated when crossing a boundary of the supertile S, using the edge marks.

2.2 Rolling graphs

Let P be a convex polyhedron in $\mathbb{R}^3$. We denote by $|P|$ the number of faces of P. The face structure of P can be represented by its dual graph G_P where each face of P is a vertex in G_P and two vertices are connected by an edge if the two corresponding faces of P share an edge (Figure 14).

For a face $f \in P$ or a tile $t \in T$, denote by $|f|$ and $|t|$ its number of edges. We number the edges of every face f of polyhedron P counter-clockwise starting from one arbitrary edge that will serve as the reference edge. We do the same for every tile t of the supertile S (and the corresponding tessellation T), with one edge being the reference edge, and the next edges being numbered in clockwise order. A face $f \in P$ is *compatible* with $t \in T$ in the *orientation* o if $|f| = |t|$ and the counter-clockwise sequence of edge lengths and angles in f starting at edge number o matches exactly the clockwise sequence of edge lengths and angles in t starting from the reference edge. This means that f can be placed in the plane with edge number o overlapping with the reference edge of t so that the two polygons overlap perfectly.

We say polyhedron P *sits on the tile t in the tessellation T with its face f at orientation o* if f and t completely overlap and the edge number o of f overlaps the reference edge of t. The *position* of P is then represented by the tuple $\langle t, f, o\rangle$. When T is a periodic tiling with supertile S, and $t = \langle (i,j), s\rangle$ for $s \in S$, then this position can be written as $\langle (i,j), s, f, o\rangle$. The *state* associated with this position is the tuple $\langle s, f, o\rangle$.

The *rolling graph* $G_{P,T}$ for P and T is an infinite graph whose vertex set is the set of all possible positions $\langle t, f, o\rangle$, and two nodes are connected by an edge if there is a valid roll between them. The positions adjacent to $\langle t, f, o\rangle$ can be easily explored by using the dual graphs of P and T. We write $\langle t, f, o\rangle \sim \langle t', f', o'\rangle$ if the two positions are connected by a path in the rolling graph. In that case, we say that the two positions are *reachable* from one another.

2.3 Symmetries of rolling graphs

In this section, we show that any large connected subgraph of the rolling graph $G_{P,T}$ has a translational symmetry. We start by bounding the number N of possible states $\langle s, f, o\rangle$ of a

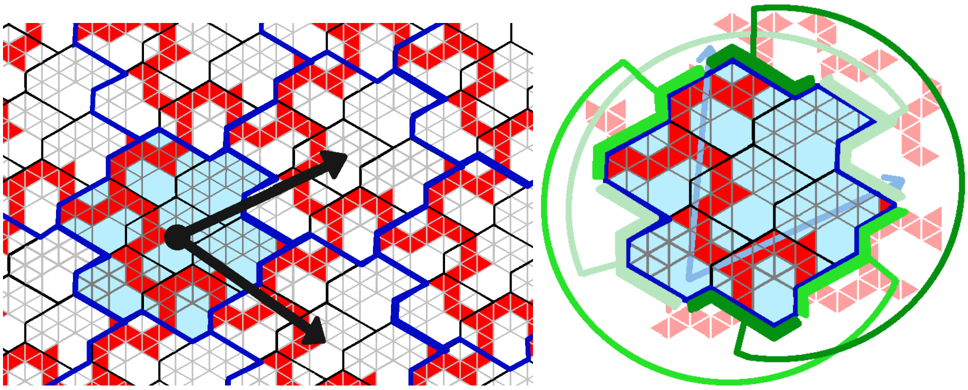

Figure 16 By finding the symmetry vectors in a connected component, we can describe a compact representation of the connected component's periodic graph (over the rolling graph).

rolling graph.

$$N = \sum_{s\in S}\sum_{f\in P}(\text{number of compatible orientations between } f \text{ and } s)$$
$$\leq \sum_{s\in S}\sum_{f\in P}|f| \leq 6|S||P|.$$

Note that the rolling graph in itself has the same translational symmetries as the tiling T, because the validity conditions are the same in both positions.

▶ **Fact 1.** *If $\langle(i,j),s_0,f_0,o_0\rangle$ has a valid roll to $\langle(i{+}i_1,j{+}j_1),s_1,f_1,o_1\rangle$, then $\langle(i',j'),s_0,f_0,o_0\rangle$ has a valid roll to $\langle(i'+i_0,j'+j_0),s_1,f_1,o_1\rangle$ for all $i',j'\in\mathbb{Z}$.*

This however does not mean that the same symmetries apply to the connected components of the rolling graph, that is, $\langle(i,j),s_0,f_0,o_0\rangle$ and $\langle(i',j'),s_0,f_0,o_0\rangle$ might not be reachable, even if the connected components are infinite. However, the following lemma shows that if two distinct reachable positions have the same state, then we obtain a translational symmetry on their connected components in the rolling graph.

▶ **Lemma 1.** *If $\langle(i,j),s,f,o\rangle \sim \langle(i+u,j+v),s,f,o\rangle$ then $\forall\langle(i',j'),s',f',o'\rangle \sim \langle(i,j),s,f,o\rangle$, $\langle(i',j'),s'f',o'\rangle \sim \langle(i'+u,j'+v),s',f',o'\rangle$.*

That is, $u\vec{a}+v\vec{b}$ defines a translational symmetry on the connected component of $\langle(i,j),s,f,o\rangle$ in the rolling graph.

Proof. Write the path from $\langle(i',j'),s',f',o'\rangle$ to $\langle(i,j),s,f,o\rangle$ in the rolling graph as $\langle(i,j),s,f,o\rangle = \langle(i+i_0,j+j_0),s_0,f_0,o_0\rangle,\dots,\langle(i+i_k,j+j_k),s_k,f_k,o_k\rangle = \langle(i',j'),s',f',o'\rangle$. Since, by Fact 1, $\langle(i+u+i_\ell,j+u+j_\ell),s_\ell,f_\ell,o_\ell\rangle$ to $\langle(i+u+i_{\ell+1},j+u+j_{\ell+1}),s_{\ell+1},f_{\ell+1},o_{\ell+1}\rangle$ is a valid roll, we can construct the path $\langle(i',j'),s',f',o'\rangle = \langle(i+i_k,j+j_k),s_k,f_k,o_k\rangle,\dots,\langle(i+i_0,j+j_0),s_0,f_0,o_0\rangle = \langle(i,j),s,f,o\rangle \sim \langle(i{+}u,j{+}v),s,f,o\rangle = \langle(i{+}u{+}i_0,j{+}v{+}j_0),s_0,f_0,o_0\rangle,\dots\langle(i+u+i_k,j+v+j_k),s_k,f_k,o_k\rangle = \langle(i'+u,j'+v),f',o'\rangle$ ◀

▶ **Lemma 2.** *There is an algorithm which, in $O(|P||S|)$ time either finds a base of the translational symmetries of the connected component of the rolling graph containing a given position $\langle(i,j),s,f,o\rangle$, or decides that the connected component is of finite size.*

Proof. Run a depth first search on the rolling graph starting from $\langle(i,j),s,f,o\rangle$, for N steps. If the depth first search stops, then the connected component containing $\langle(i,j),s,f,o\rangle$ in the rolling graph is of finite size. Otherwise, by the pigeonhole principle, we have found two positions with the same state. By Lemma 1, we obtain a translational symmetry $u\vec{a} + v\vec{b}$ of the connected component.

Next, factor the rolling graph by this symmetry vector, that is, $G_{P,T}/\{u\vec{a} + v\vec{b}\}$ identifies any pair of positions $\langle(i,j), s, f, o\rangle$ and $\langle(i+ku, j+kv), s, f, o\rangle$ for all $k \in \mathbb{Z}$. Run again a depth first search in $G_{P,T}/\{u\vec{a} + v\vec{b}\}$ starting from $\langle(i,j), s, f, o\rangle$, for N steps. If the depth first search stops, then there are only a finite number of orbits for this symmetry vector, and so only one translational symmetry in this connected component. Otherwise, again by the pigeonhole principle and Lemma 1, we have found a second linearly independent translational symmetry $u'\vec{a} + v'\vec{b}$ for this connected component. ◀

The algorithm in the above lemma finds a basis of two, one or zero translational symmetries in the connected component. We can factor the rolling graph by those symmetries by identifying symmetric tiles. As the symmetries are multiples of the supertile symmetries, this is easily done by performing a coordinate change from the (i,j) coordinates to coordinates in the new basis, **and a modulus operation.** When there is no symmetry, the algorithm identifies a bounded connected component in $G_{P,T}$. When there is one symmetry vector, the algorithm finds a finite number of orbits for this symmetry. Finally, when there are two symmetry vectors in the basis, the factored rolling graph $G_{P,T}/\{u\vec{a} + v\vec{b}, u'\vec{a} + v'\vec{b}\}$ is of size polynomial in N and the connected component can be explored completely by depth first search. In all three cases, a compact representation of the connected component has been found. In the two latter cases, it takes the form of a polynomially-sized fundamental domain and one or two translational symmetry vectors.

2.3.1 Results on reachability

The arguments above show how to identify the connected components in the rolling graph. In order to find the set of tiles that can be reached from a starting position, we only need to look at the first part $(i,j), s$ of the positions in the connected component. Because this is a projection, it preserves the symmetry vectors. We obtain the following classification for the reachable area.

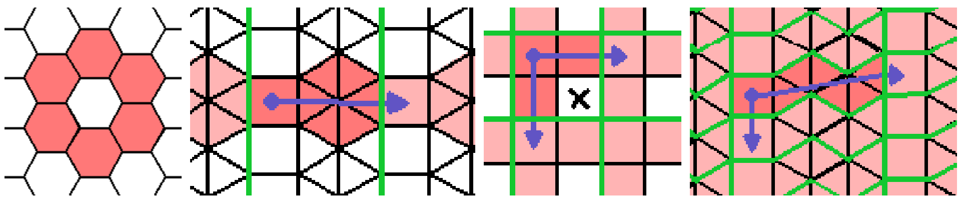

Figure 17 No vector, one vector, two vectors but fail to cover, two vectors and full cover.

- If the rolling graph does not have symmetry vectors, the reachable area is bounded and P on T starting at $\langle t, f, o\rangle$, is a *bounded roller.*
- If the rolling graph only has one linearly independent vector, the reachable area is a band and P on T starting at $\langle t, f, o\rangle$ is a *band roller.*
- If the rolling graph has two linearly independent vectors, the reachable area extends infinitely in all directions. If not every tile t is present in the reachable supertiles, the reachable tiles forms a plane with holes and P on T starting at $\langle t, f, o\rangle$ is a *hollow-plane roller.*

- If every tile t is present in the reachable supertiles, the reachable tiles cover the entire plane and P on T starting at $\langle t, f, o\rangle$ is a *plane roller*.

3 Considerations for usage in puzzles

To make a rolling puzzle game, we need at least: a playing area with obstacles and paths; a polyhedron that will navigate that space; departing from a starting point; and arriving at a goal point. The goal is often matching a specific face with a specific tile. After selecting a polyhedron and a tessellation that have a useable reachable area pattern, we identify several additional properties that should be tracked to facilitate puzzle design.

3.1 Useful properties

Unused tiles in the playing area.

This is determined by the reachable area of the roller. The puzzle designer should not put interactive elements on tiles that cannot be reached. The puzzle designer would use the representative area and its symmetries to map out the playing space.

Unused faces on the polyhedron.

For face-matching puzzles, determining which faces of the polyhedron are usable in the puzzle is also important. Some faces might not be compatible with the tiling, while others might not appear in the connected rolling graph despite being compatible. For example, puzzle designers should avoid putting an objective marker on a polyhedron face that cannot be rolled on. Which face was used or not is additional information that should be tracked when computing the reachable area.

Guaranteed starting point: stability.

In order to use a plane roller, we must know one state corresponding to the connected part of the rolling graph that covers the plane. By starting from the wrong state (wrong face or orientation), we might not be in a component that is connected to the one that covers the whole plane. For some rollers, some tiles are guaranteed to belong to the largest component for every compatible state on which we start. We can track and mark those tiles while computing the reachable area, as those tiles can serve as starting positions to ensure that our polyhedron will roll the plane. We call this property *tile stability*. Puzzle designers should put the starting position of the polyhedron on a stable tile to guarantee plane coverage.

▶ **Definition 3.** *A plane roller pair* (P, T) *is* stable *on a tile* $t \in T$ *if*

$$\forall f \in P \quad s.t. \quad |f| = |t|, \quad \forall o \in f : P, T \text{ on } \langle t, f, o\rangle \text{ is a roller.} \tag{1}$$

▶ **Definition 4.** *The reachable area RA for a rolling pair* P, T *is* stable *on a tile* $t \in T$ *if*

$$\forall f \in P \quad s.t. \quad |f| = |t|, \quad \forall o \in f : \forall t_i \in RA : \exists f_i, o_i \quad s.t. \quad \langle t, f, o\rangle \sim \langle t_i, f_i, o_i\rangle \tag{2}$$

Which face reaches which tile: face-completeness.

In a face-matching rolling puzzle game, the objective is to reach a specific tile with a specific face on the polyhedron (often marked by a different color). In some cases, not every face of a particular shape can reach every tile. When using a polyhedron/tiling pair in a puzzle game, it can help to know which face can reach which tile. We can track specific tiles that can be reached by every compatible face during our computations. We call those tiles face-complete tiles. Refer to Figure 18.

▶ **Definition 5** (face-complete tile). *A roller for P on T at $\langle t_0, f_0, o_0 \rangle$ has a face-complete tile $t \in T$ iff all compatible faces of the polyhedron can roll on t with some orientation, that is,* $\forall f \quad s.t. \quad |t| = |f| : \exists o \quad s.t. \quad \langle t, f, o \rangle \sim \langle t_0, f_0, o_0 \rangle$.

▶ **Definition 6** (face-orientation-complete tile). *A* face-orientation-complete *tile is one that can be visited with all compatible faces in every orientation within a connected component.*

3.2 Puzzlemaker's reference image

We combined all the above results in one image as a reference point for puzzlemakers. This allows to select a tessellation/polyhedron pair very easily depending on the puzzle's needs.

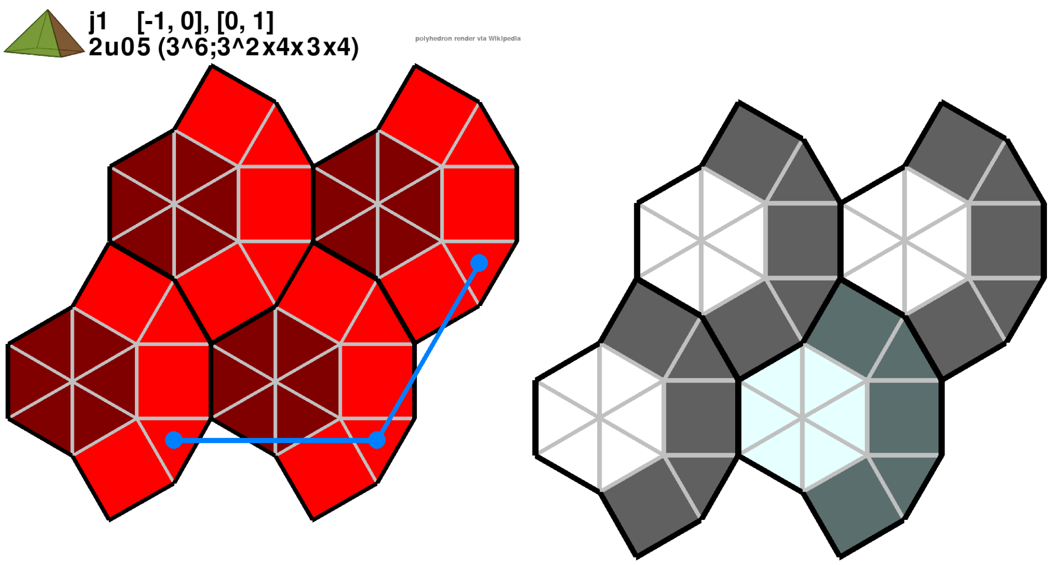

Figure 18 Left: face-completeness graph. In brown: face-complete tiles. In red: face-orientation-complete. Right: Stability graph with stable tiles in grey.

4 Implementation

The algorithm was implemented in Python 3.8 and is available on GitHub at `https://github.com/akirbaes/RollingPolyhedron/blob/master/RollingProof.py`. It uses NumPy and SymPy for creating a minimal linearly independent base, and pygame to produce images.

The implemented version performs further manipulations, such as aggregating connected rolling graph states grouped by supertile into superstates, to lower processing time and avoid dealing with individual tile positions calculations by only looking at the supertile cartesian coordinates.

The result table can be consulted at `https://akirabaes.com/polyrolly/resulttable/`.

5 Limitations

It is left to prove for the 87 polyhedrons out of the 129 considered that did not generate a plane roller with the 131 considered tilings, if there doesn't exist a tiling on which they would be able to roll on the 2D plane.

dodecahedron, truncated cube, truncated octahedron, rhombicuboctahedron, truncated cuboctahedron, snub cube, snub cube c, icosidodecahedron, truncated dodecahedron, truncated icosahedron, rhombicosidodecahedron, truncated icosidodecahedron, snub dodecahedron, snub dodecahedron c, j2, j4, j5, j6, j7, j9, j18, j19, j20, j21, j23, j24, j25, j32, j33, j34, j35, j36, j38, j39, j40, j41, j42, j43, j45, j45 c, j46, j46 c, j47, j47 c, j48, j48 c, j49, j52, j53, j55, j57, j58, j59, j60, j61, j63, j64, j66, j67, j68, j69, j70, j71, j72, j73, j74, j75, j76, j77, j78, j79, j80, j81, j82, j83, j91, j92, triangular prism, pentagonal prism, hexagonal prism, octagonal prism, decagonal prism, dodecagonal prism, pentagonal antiprism, octagonal antiprism, decagonal antiprism, dodecagonal antiprism

Table 2 Considered polyhedrons which did not generate a plane roller with considered tilings

Acknowledgements

Part of this work appeared in the first author's Master's Thesis.

Part of this work was done at the 35th Bellairs Winter Workshop on Computational Geometry (Online). The authors would like to thank all participants.

Part of this work was done at the Barbados 2020 summer Workshop on Computational Geometry (Online). The authors would like to thank all participants.

Renders of prisms and antiprisms must be attributed to Stella software as per license. Other polyhedron renders from Wikimedia Commons are to be attributed to their respective creators.